Journal of Thermal Analysis and Calorimetry, Vol. 67 (2002) 535–546

PHASE DIAGRAM AND GROWTH BEHAVIOUR OF DURENE–RESORCINOL SYSTEM

U. S. Rai and P. Pandey

Chemistry Department, Banaras Hindu University, Varanasi, 221 005 (U. P.) India

(Received April 5, 2001; in revised form June 27, 2001)

Abstract

Phase diagram of durene–resorcinol system, determined by the thaw-melt method, shows the formation of a monotectic (0.109 mole fraction of durene) and an eutectic (0.964 mole fraction of durene) with a large liquid miscibility gap in the region from 0.109 to 0.964 mole fraction of durene. The eutectic, monotectic and consolute temperatures are 78.4, 107.8 and 165.0°C, respectively. The growth behaviour studied by measuring the linear velocity of crystallization (v) in a capillary at different undercoolings (ΔT) suggests that the data obey the Hillig–Turnbull equation, $v=u(\Delta T)^n$, where u and n are constants depending on the nature of materials involved. From the values of enthalpy of fusion of the pure components, the eutectic and the monotectic determined by the DSC method using Mettler DSC-4000 system, entropy of fusion, enthalpy of mixing, Jackson's roughness parameter, size of the critical nucleus interfacial energy and excess thermodynamic functions were calculated. The microstructures of the eutectic, and the monotectic, determined by the Leitz Laborlux D optical microscope show their characteristic features.

Keywords: growth kinetics, organic monotectic, phase-diagram, thermochemistry

Introduction

The evergrowing demand of newer materials to meet the needs of modern civilization has put excessive pressure on chemists, physicists and metallurgists to develop these materials with specific properties at low cost. The past few decades recorded immense interest in understanding the fundamentals [1–4] of solidification process and properties of polyphase alloys. The physical chemistry of eutectics [5], monotectics [6] and intermetallic compounds [7] has been a field of active investigation due to their unusual physical properties, normally not exhibited by the parent components. Metallic eutectics, monotectics and intermetallic compounds constitute an interesting area of investigation [8, 9] in metallurgy and materials science. However, the transparent binary alloy models [10–12] are of special importance to metallurgists and materials scientists as they permit visual observation of phase transformations and the processes occurring during solidification. Low transformation temperature, ease of purification, transparency, minimised convection effects and wider choice of materi-

1418–2874/2002/ $ 5.00

Akadémiai Kiadó, Budapest
Kluwer Academic Publishers, Dordrecht

als are the special features which have prompted a number of research groups [10–12] to undertake some physicochemical studies on organic eutectics, monotectics and addition compounds. Furthermore, the organic systems are more suitable for a detailed study of the parameters controlling the solidification process because the experimental techniques required for these investigations are simplier and more convenient as compared to those adopted for metallic systems.

Most of the organic systems studied in the past are of simple eutectic type. There are only few systems in which two components form either a monotectic with large miscibility gap or an addition compound with congruent melting point. Durene (enthalpy of fusion=19.4 kJ mol^{-1}) and resorcinol (enthalpy of fusion=21.0 kJ mol^{-1}) are high enthalpy of fusion compounds and as such a system consisting of durene (D) and resorcinol (RES) is an organic analogue of a non-metal-non-metal system. Phase diagram, growth behaviour, thermochemistry and microstructure of this system are reported in the present investigation.

Experimental

Materials and purification

While durene obtained from Fluka, Switzerland was purified by recrystallizing it 3–4 times, resorcinol (Merck, India) was purified by repeated distillation under reduced pressure and stored in amber coloured bottles to avoid exposure to light. The melting point of pure durene and resorcinol were found to be 80.3 and 110.5°C, respectively, which are close to their respective literature values 80.0 and 110.0°C.

Phase diagram

The phase diagram of a system [11–13] is studied to know the accurate composition and melting point of eutectics and monotectics. Different mixtures of the two organic compounds taken in different propositions by mass covering the entire range of composition were prepared in long necked test tubes. After sealing the test tubes, these mixtures were homogenized for about 4–5 times, by repeating the process of melting in silicone oil followed by chilling the mixtures in ice. The temperature corresponding to the onset of melting is recorded as thaw temperature, and the temperature at which melting is complete is recorded as melting temperature.

Growth kinetics

The linear velocity of crystallization was determined [14] in a U-form capillary tube by measuring the rate of movement of the solid–liquid interface at different undercoolings. The growth velocity was measured with the help of a travelling microscope and a stopwatch.

Enthalpy of fusion

The values of enthalpy of fusion of the pure components the eutectic and the monotectic were determined [15–16] by the DSC method using Mettler DSC-4000 system. The apparatus was calibrated using indium as standard sample. To confirm the accuracy of the instrument, enthalpy of fusion of benzoic acid was also determined and the value was compared with the literature value. The amount of sample and heating rate were about 5 mg and 10°C min^{-1}, respectively.

Microstructure

The microstructure of each of the pure components, eutectic and monotectic was determined [17] by placing a small amount of sample on a well washed and dried glass slide in an oven maintained at a temperature slightly above the melting point of the sample. On complete melting a coverslip is glided over the melt and after a few minutes the supercooled melt was nucleated by the solid of same composition and then it was subjected to unidirectional solidification. After complete solidification, the solid was placed on the platform of a Leitz Laborlux D, optical microscope and the different interesting regions were photographed.

Results and discussion

Phase diagram

Phase diagram of durene–resorcinol system is given in Fig. 1 in the form of composition-temperature plots. Melting point of resorcinol is 110.5°C which decreases with increasing mole fraction of durene. At the monotectic temperature 107.8°C, corresponding to 0.109 mole fraction of durene, two liquid phases and a solid phase appear. At this composition when liquid L_1 is cooled below this temperature, another liquid and a solid phase appear according to the following reaction:

$$L_1\ (\text{liquid rich in resorcinol}) \rightarrow L_2\ (\text{liquid rich in durene}) + S_1\ (\text{solid rich in resorcinol})$$

This is the monotectic [18] reaction of the durene–resorcinol system. In the region from 0.109 to 0.964 mole fraction of durene and above the monotectic temperature two immiscible liquids L_1 and L_2 coexist. At the eutectic temperature, 78.4°C (0.964 mole fraction of durene), liquid rich in durene L_2 is in equilibrium with two solid phases and below this temperature the following reaction takes place:

$$L_2\ (\text{liquid rich in durene}) \rightarrow S_1\ (\text{solid rich in resorcinol}) + S_2\ (\text{solid rich in durene})$$

Thus, the monotectic reaction at 107.8°C is quite similar to the eutectic reaction taking place at 78.4°C except that one of the resultant phases is liquid. In the area recorded as RES(S)+D(L_2) solid resorcinol and liquid durene coexist and in the area mentioned as RES(S)+D(S) two solid phases coexist. If we draw a number of the tie lines between curves MC and M_hC running parallel to the X-axis (constituting mole fraction of durene) in the L_1 L_2 region these lines become progressively [6] smaller

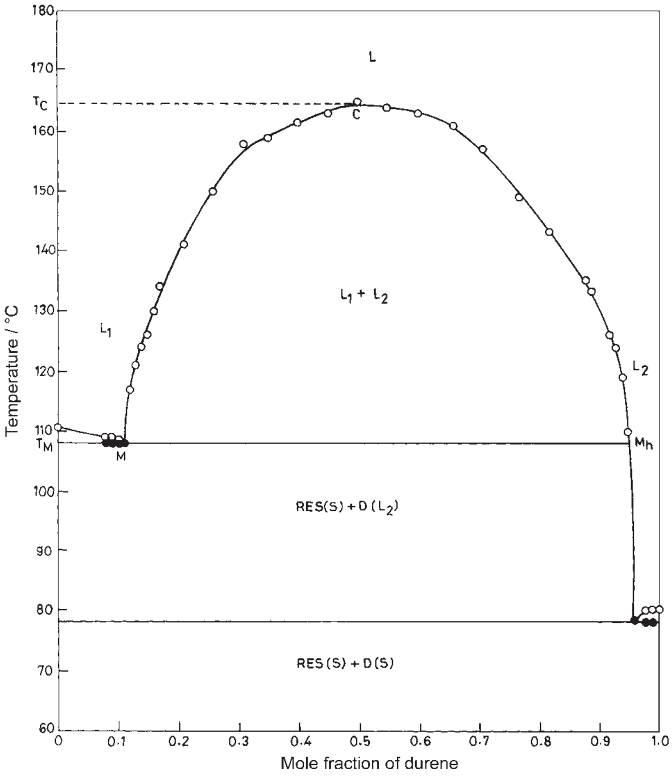

Fig. 1 Phase diagram of durene–resorcinol system: (o) melting temperature; (•) thaw temperature

until a point at 165.0°C is reached. This is the consolute temperature of the system which is 57.2°C above the monotectic horizontal. Above this temperature only one liquid phase exists in the entire range of composition.

Growth kinetics

The values of linear velocity of crystallization of pure compounds, eutectic and monotectic were determined at different undercoolings by measuring the rate of movement of solid–liquid interface in a capillary. According to Hillig and Turnbull [19], the growth rate, v, is related to undercooling by the expression.

$$v = u(\Delta T)^{n} \tag{1}$$

where u and n are constants depending on the nature of materials.

The variation of growth velocity at different undercoolings is shown in Fig. 2 in the form of linear plots with $\log\Delta T$ on X-axis and $\log v$ on Y-axis. The values of u and n determined from the plots are given in Table 1. The basic criteria for the determina-

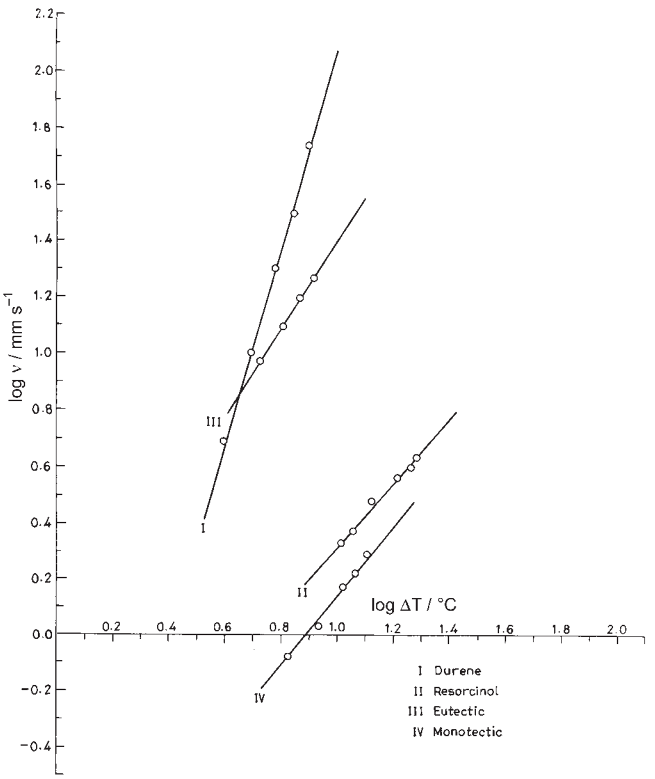

Fig. 2 Linear velocity of crystallization of durene, resorcinol, their eutectic and monotectic

tion of growth mechanism [20] is the comparison of temperature dependence of the linear velocity of crystallization with the theoretically predicted equations. Normal growth generally occurs on rough interface and for this there is direct proportionality between growth velocity and undercooling. Lateral growth is facilitated by the presence of steps, jogs, bends etc. and under such conditions, the relationship for the spiral mechanism follows the parabolic law given by Eq. (1). The values of u which give a measure of the rate of crystallization are also given in Table 1. It can be inferred from the values reported in the table that the growth velocity of durene is higher than that of resorcinol. The growth rate of eutectic is more than the two components while it lies between the two components in the case of monotectic. The velocity of the eutectic is roughly ten times more than that of the monotectic. This difference may be attributed to the different mode of conduction of heat and mode of diffusion of molecules in the eutectic and monotectic phases during the crystallization process. The lower growth rate of eutectic and monotectic is due to the side-by-side growth of the two phases involved.

Table 1 Value of u and n for pure components, eutectic and monotectic

Material	u/mm s^{-1} K^{-1}	n
Durene (D)	$2.8\cdot10^{-2}$	3.6
Resorcinol (RES)	$1.4\cdot10^{-1}$	1.2
D–RES eutectic	$7.1\cdot10^{-1}$	1.5
D–RES monotectic	$7.0\cdot10^{-2}$	1.3

It is well known that when a liquid is cooled below its equilibrium melting temperature, the liquid phase does not solidify spontaneously, because under equilibrium conditions, it contains clusters of molecules. As long as the clusters are well below the critical size [21], they cannot grow to form a crystal and no solid is formed. The interfacial energy (σ) is related [22] to the critical radius (r^*) of the nucleus by the equation,

$$r^* = \frac{2\sigma T_\mathrm{m}}{\Delta H_\mathrm{f}\Delta T} \tag{2}$$

where T_m, ΔH_f and ΔT are the melting temperature, heat of fusion and degree of undercooling, respectively. The interfacial energy is given by the expression [22],

$$\sigma = \frac{C\Delta H_\mathrm{f}}{(N)^{1/3} V_\mathrm{m}^{2/3}} \tag{3}$$

where N is the Avogadro number, V_m is the molar volume, and parameter C lies between 0.30 to 0.35.

The values of interfacial energy, calculated by using Eq. (3) are given in Table 2. The critical radius of the nucleus for pure components, the eutectic and the monotectic was calculated using Eqs (2) and (3) and the values are given in Table 3. It is clear from the data that for a given sample, the size of critical nucleus decreases with the increase in undercooling. The undercooling of the interface provides [23] the driving force for the kinetic process in the direction of freezing, and its magnitude decides the rate of growth. In addition, at increased undercooling the bulk free energy available for the phase transformation is increased, thereby lowering the total barrier height for nucleation. Consequently, smaller thermodynamic fluctuations can, with statistical certainty, eventually form a viable nucleus of size greater than the critical.

Table 2 Interfacial energy values for durene, resorcinol and their monotectic

Parameters	Value/erg cm^{-2}
SL_1 (D)	30.7
SL_2 (RES)	50.1
L_1L_2 (D–RES)	2.4

Table 3 Radius of critical nucleus at different degrees of undercoolings

Undercooling, ΔT/°C	Critical radius/10^{-8} cm			
	D	RES	eutectic	monotectic
4.3	2.6	–	–	–
5.3	2.1	–	–	–
5.4	–	–	2.0	–
6.3	1.8	–	–	–
6.4	–	–	1.7	–
6.8	–	–	–	2.9
7.3	1.5	–	–	–
7.4	–	–	1.4	–
8.3	1.3	–	–	–
8.4	–	–	1.3	–
8.8	–	–	–	2.3
10.5	–	1.7	–	–
10.8	–	–	–	1.9
11.5	–	1.6	–	–
11.8	–	–	–	1.7
12.8	–	–	–	1.6
13.5	–	1.4	–	–
16.5	–	1.1	–	–
18.5	–	1.0	–	–
19.5	–	0.9	–	–

Thermochemistry

The values of enthalpy of fusion of the pure components, the eutectic and the monotectic give idea about the mechanism of crystallization, microstructure, structure of eutectic melt and the nature of interaction between two components forming the polyphase alloys. The experimental values of the enthalpy of fusion, determined by the DSC method, are reported in Table 4; the percentage error in the values being ±1.0. For the purpose of comparison their calculated values are also given in the same table. If the eutectic is a simple mechanical mixture of the two components involving neither heat of mixing nor any type of association in the melt, the heat of fusion can simply be given by the mixture law [24],

$$(\Delta_{\mathrm{f}} h)_{\mathrm{e}} = x_1 \Delta_{\mathrm{f}} h_1^0 + x_2 \Delta_{\mathrm{f}} h_2^0 \tag{4}$$

where x and $\Delta_{\mathrm{f}} h$ are the mole fraction and heat of fusion respectively, of the component indicated by the subscript.

Table 4 Heat of fusion, entropy of fusion and Jackson's roughness parameter

Material	Heat of fusion/ kJ mol^{-1}	Entropy of fusion/ J mol^{-1} K^{-1}	Roughness parameter/ $\alpha=\Delta_f S/R$
Durene (D)	19.4	55.0	6.6
Resorcinol (RES)	21.0	54.8	6.6
D–RES eutectic (experimental)	20.8	59.1	7.1
D–RES eutectic (calculated)	19.5	–	–
D–RES monotectic (experimental)	18.3	54.8	6.6

When a solid eutectic melts, there is considerable possibility of association and heat of mixing, both causing violation of the mixture law. It is evident from the data in the table that the calculated value is higher than the experimental one by 1.3 kJ. This value is equal to the enthalpy of mixing which is given by the difference in the experimental and calculated values of enthalpy of fusion of the eutectic. Thermochemical studies [25] suggest that the structure of a binary eutectic melt depends on the sign and magnitude of heat of mixing. As such, three types of structures are suggested; quasi-eutectic for $\Delta_m H>0$, clustering of molecules for $\Delta_m H<0$ and molecular solution for $\Delta_m H=0$. The positive value of $\Delta_m H$ suggests a quasi-eutectic structure of binary eutectic melt in the present case. Entropy of fusion, calculated by dividing the enthalpy of fusion of a material by its melting temperature on absolute scale being highly positive in all the cases (Table 4) suggests that the entropy favours the melting process of eutectics and components.

The deviation from ideal behaviour can be best expressed in terms of excess thermodynamic functions [26], which gives a quantitative idea about the nature of molecular interactions. The difference between the thermodynamic functions of mixing for a real system and the corresponding values for an ideal system at the same temperature and pressure is called the excess thermodynamic functions. It is denoted by superscript E and represents the excess (positive or negative) of a given thermodynamic property of a solution over that in the ideal (reference) solution

$$Y=\Delta Y_{\text{mix}}(\text{real}) - \Delta Y_{\text{mix}}(\text{ideal}) \tag{5}$$

where Y can be taken as any of the thermodynamic functions.

In order to know the nature of interaction between the components forming the eutectic melt, some thermodynamic functions such as excess free energy (g^E), excess enthalpy (h^E) and excess entropy (s^E) were calculated using the following equations [27]:

$$g^E=RT(x_1\ln\gamma_1^1+x_2\ln\gamma_2^1) \tag{6}$$

$$h^{\mathrm{E}}=-RT^{2}\left(x_{1}\frac{\partial\ln\gamma_{1}^{1}}{\partial T}+x_{2}\frac{\partial\ln\gamma_{2}^{1}}{\partial T}\right) \tag{7}$$

$$s^{\mathrm{E}}=-R\left(x_{1}\ln\gamma_{1}^{1}+x_{2}\ln\gamma_{2}^{1}+x_{1}T\frac{\partial\ln\gamma_{1}^{1}}{\partial T}+x_{2}T\frac{\partial\ln\gamma_{2}^{1}}{\partial T}\right) \tag{8}$$

In order to calculate the excess functions, the activity coefficient and its variation with temperature are required. The activity of a component present in the eutectic melt is given by

$$-\ln x_{\mathrm{i}}^{1}\gamma_{\mathrm{i}}^{1}=\frac{\Delta_{\mathrm{f}}h_{\mathrm{i}}^{0}}{R}\left(\frac{1}{T}-\frac{1}{T_{\mathrm{i}}^{0}}\right) \tag{9}$$

where x_{i}^{1}, γ_{i}^{1}, $\Delta_{\mathrm{f}}h_{\mathrm{i}}^{0}$ and T_{i}^{0} are the mole fraction, activity coefficient, heat of fusion and melting temperature of the component *i*, respectively, *R* is the gas constant and *T* is the melting temperature of the eutectic.

Equation (9) is obtained by assuming the general condition of phase equilibrium for the phase and that heat of fusion is independent of temperature and the two components are miscible in the liquid phase only. The values of $\partial\ln\gamma_{2}^{1}/\partial T$ can be deter-

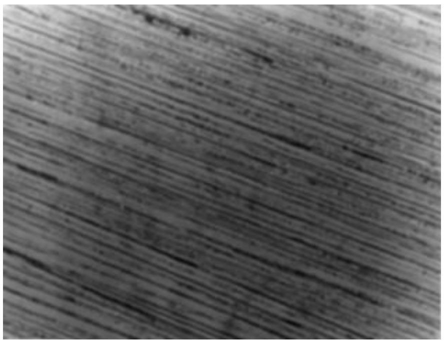

Fig. 3 Microstructure of monotectic; ×500

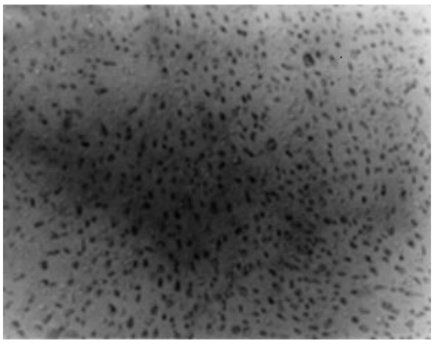

Fig. 4 Microstructure of eutectic; ×500

mined [27] by taking the slope of the liquidus curve near the eutectic point in the phase diagram and using Eq. (10) which is obtained on differentiating the Eq. (9),

$$\frac{\partial \ln \gamma_i^1}{\partial T} = \frac{\Delta_f h_i^0}{RT^2} = \frac{1}{x_i}\frac{\partial x_i}{\partial T} \tag{10}$$

Since the liquidus curves in phase diagram are virtually straight lines in the region of the eutectic composition, the values of $\partial x_i/\partial T$ has been found out by measuring their slope near the eutectic point. The values of excess functions calculated in the above manner are reported in Table 5. The value of g^E being highly positive suggests [28] that there is strong association between like molecules. Thus D–D and RES–RES association is stronger than that in D–RES. The positive values of h^E and s^E correspond to g^E and are measure of excess enthalpy of mixing and excess entropy of mixing, respectively.

Table 5 Excess thermodynamic functions for the eutectic

Material	g^E/J mol^{-1}	h^E/J mol^{-1}	s^E/J mol^{-1} K^{-1}
D–RES entectic	289.1	35.7	100.8

Microstructure

In general, properties of materials are functions of their structure, and the microstructure which gives shape, size and distribution of grains in a single phase material and shape, size and distribution of phases in a polyphase material, has been found significantly important in deciding its mechanical, electrical, magnetic and optical properties. Desired type of microstructure [29], generating required properties, can be had by controlling the solidification process, addition of small amount of impurities and selecting appropriate combination of materials, besides other variables, e.g., entropy of fusion, the structure of solid liquid interface and the undercooling which have a pronounced effect on the microstructure of alloys.

Growth morphology, developed by an eutectic system during solidification, depends on the growth characteristics of individual constituent phases on the basis of which they solidify either with faceted or non-faceted interface. This behaviour is related to the nature of solid–liquid interface and can be predicted from the values of their entropy of fusion. According to Hunt and Jackson [30], the type of growth from an eutectic melt depends upon a factor α, defined as:

$$\alpha = \xi\frac{\Delta_f h}{RT} = \xi\frac{\Delta_f s}{R} \tag{11}$$

where ξ is a crystallographic factor depending upon the geometry of molecules and has the value less than or equal to 1, $\Delta_f S/R$, also known as Jackson's roughness parameter (Table 4), is entropy of fusion in dimensionless unit and R is the gas constant.

If $\alpha<2$, the solid–liquid interface is atomically rough, many sites are reacting and are continuously available for molecular attachment during growth. If $\alpha>2$, the solid–liquid interface is atomically smooth and advances into the liquid by the propagation of molecular steps across the interface.

It is evident from the microstructure of the monotectic given in Fig. 3, that there is an alignment of seed phase (1) in the direction of growth. However, there is discontinuity in the morphology of the phase. This is evidenced by the tendency of the phase to break periodically and tendency to spherodise. The microstructure of the eutectic in Fig. 4 shows particulate type of morphology. The microstructural features indicate that the second phase is distributed as particulate type of morphology in the matrix of the primary phase.

* * *

Thanks are due to UGC, New Delhi for financial assistance.

References

1 D. M. Herlach, R. F. Cochrane, I. Egry, H. J. Fecht and A. L. Greer, Int. Mater. Rev., 38 (1993) 273.
2 R. Elliot, Eutectic solidification processing, Butterworths, London 1983.
3 W. Kurz and R. Trivedi, Proc. Third Int. Conf. on Solidification Processing, Sheffield 1987, p. 1.
4 J. H. Lee and J. D. Verhoeven, J. Cryst. Growth, 143 (1994) 86.
5 Z. R. Liu, Y. H. Chao, C. M. Yin and Y. H. Kong, Thermochim. Acta, 250 (1995) 65.
6 H. Song and A. Hellawell, Metall. Trans., 20A (1989) 171.
7 W. Kurz and D. J. Fisher, Acta Metall., 29 (1981) 11.
8 S. Chaubey, K. S. Dubey and P. R. Rao, J. Alloy Phase Diagram, 6 (1990) 153.
9 J. C. Gachon, J. Phys. Chem. Solids, 49 (1988) 435.
10 J. E. Smith, D. O. Frazier and W. F. Kaukler, Scripta Metallurgica, 18 (1984) 677.
11 J. Sangster, J. Phys. Chem. Ref. Data, 23 (1994) 295.
12 U. S. Rai and R. N. Rai, J. Mater. Res., 14 (1999) 1299.
13 U. S. Rai and P. Pandey, Materials Letters, 39 (1999) 166.
14 U. S. Rai and K. D. Mandal, Bull. Chem. Soc. Japan, 63 (1999) 1496.
15 J. W. Dodd, K. H. Tonge, in B. R. Currell (ed.), Thermal Methods, Analytical Chemistry by Open Learning, Wiley, New York 1987.
16 U. S. Rai and R. N. Rai, J. Cryst. Growth, 191 (1998) 234.
17 U. S. Rai and H. Shekhar, Mol. Cryst. Liq. Cryst., 220 (1992) 217.
18 N. B. Singh, U. S. Rai and O. P. Singh, J. Cryst. Growth, 71 (1985) 353.
19 W. B. Hillig and D. Turnbull, J. Chem. Phys., 24 (1956) 91.
20 D. A. Porter and K. E. Easterling, Phase Transformaitons in Metals and Alloys, Van Nostrand Reinhold, New York 1982.
21 J. W. Christian, The Theory of Phase Transformations in Metals and Alloys, Pergamon Press, Oxford 1965.
22 U. S. Rai and H. Shekhar, Thermochim. Acta, 186 (1991) 131.
23 U. S. Rai and R. N. Rai, Chem. Materials. Am. Chem. Soc., (in press).

24 U. S. Rai and S. George, Thermochim. Acta, 243 (1994) 17.
25 N. Singh, N. B. Singh, U. S. Rai and O. P. Singh, Thermochim. Acta, 95 (1985) 291.
26 U. S. Rai, O. P. Singh, N. P. Singh and N. B. Singh, Thermochim. Acta, 71 (1983) 373.
27 U. S. Rai and S. George, J. Mater. Sci., 27 (1992) 711.
28 J. Wisniak and A. Tamir, Mixing and Excess Thermodynamic Functions. A literature sourcebook, Phys. Sci. Data, Elsevier, New York 1978.
29 G. A. Chadwick, Metallography of Phase Transformations, Butterworth, London 1972.
30 J. D. Hunt and K. A. Jackson, Trans Met. Soc. AIME, 236 (1966) 843.